Title

Transcriptional expression patterns triggered by chemically distinct neuroprotective molecules.

Authors

Pappas, DJ
Gabatto, PA
Oksenberg, D
et al.

Publication Date

2012-12-01

DOI

10.1016/j.neuroscience.2012.09.007

Peer reviewed

Neuroscience 226 (2012) 10–20

TRANSCRIPTIONAL EXPRESSION PATTERNS TRIGGERED BY CHEMICALLY DISTINCT NEUROPROTECTIVE MOLECULES

D. J. PAPPAS,[a]* P. A. GABATTO,[a] D. OKSENBERG,[a] P. KHANKHANIAN,[a] S. E. BARANZINI,[a] L. GAN[b] AND J. R. OKSENBERG[a]

[a] *Department of Neurology, University of California, San Francisco, CA, USA*

[b] *Gladstone Institute of Neurological Disease, University of California, San Francisco, CA, USA*

Abstract—Glutamate-mediated excitotoxicity has been purported to underlie many neurodegenerative disorders. A subtype of glutamate receptors, namely *N*-methyl-D-aspartate (NMDA) receptors, has been recognized as potential targets for neuroprotection. To increase our understanding of the mechanisms that underlie this neuroprotection, we employed a mouse model of glutamate receptor-induced excitotoxic injury. Primary cortical neurons derived from postnatal day-0 CD-1 mice were cultured in the presence or absence of neuroprotective molecules and exposed to NMDA. Following a recovery period, whole genome expression was measured by microarray analysis. We used a combination of database and text mining, as well as systems modeling to identify signatures within the differentially expressed genes. While molecules differed in their mechanisms of action, we found significant overlap in the expression of a core group of genes and pathways. Many of these molecules have clear links to neuronal protection and survival, including ion channels, transporters, as well as signaling pathways including the mitogen-activated protein kinase (MAPK), the Toll-like receptor (TLR), and the hypoxic inducible factor (HIF). Within the TLR pathway, we also discovered a significant enrichment of interferon regulatory factor 7 (IRF7)-regulated genes. Knockdown of *Irf7* by RNA interference resulted in reduced survival following NMDA treatment. Given the prominent role that IRF7 plays in the transduction of type-I interferons (IFNs), we also tested whether type-I IFNs alone functioned as neuroprotective agents and found that type-I IFNs were sufficient to promote neuronal survival. Our data suggest that the TLR/IRF7/IFN axis plays a significant role in recovery from glutamate-induced excitotoxicity.

Key words: neuron, glutamate, NMDA, excitotoxicity, neuroprotection, microarray.

INTRODUCTION

Deregulation of glutamate homeostasis within the central nervous system and the resultant excitotoxic injury has been linked to the pathological mechanisms that ensue after cerebral ischemia and trauma and potentially underlie complex neurodegenerative disorders (Sheldon and Robinson, 2007; Dong et al., 2009). However, despite decades of research and promising data from both *in vitro* experiments and clinical trials, efforts on specific therapeutic targeting of ionotropic glutamate (*N*-methyl-D-aspartate (NMDA)–AMPA–Kainate) receptors have been largely unsuccessful (Villmann and Becker, 2007; Besancon et al., 2008). The clinical shortcomings of targeting NMDA receptors may be due to poor relevance of animal models or suboptimal design of clinical trials (Hoyte et al., 2004). The disconnect may also arise from an oversimplified standard model of excitotoxicity, which links cell death to a linear cascade of signaling events following receptor overstimulation (Besancon et al., 2008). For example, NMDA receptors (NMDA-R) may stimulate cell survival or cell death signals, depending on their subcellular localization. Whereas extra-synaptic NMDA-R activation may preferentially trigger cell death cascades, synaptic NMDA-R activation may promote neuroprotection, (Hardingham and Bading, 2010). The release of axonal glutamate can be preceded by large Na^+ influxes which have been suggested to be more detrimental than the ultimate Ca^{2+} imbalance of the standard model (Besancon et al., 2008). Moreover, an expanded repertoire of glutamate and Ca^{2+} sensing receptors and transporters in the CNS continues to unfold (Villmann and Becker, 2007; Besancon et al., 2008; Trapp and Stys, 2009). Neuroprotective agents may have multiple mechanistic roles in neuroprotection. For example Riluzole, an FDA approved therapeutic for the treatment of amyotrophic lateral sclerosis (ALS), has been proposed to act as an antagonist of both glutamate receptors and glutamate transporters (Villmann and Becker, 2007), in addition to a tetrodotoxin-sensitive sodium channel blocker (Song et al., 1997), and a two-

*Corresponding author. Address: 675 Nelson Rising Lane, Room 240, San Francisco, CA 94158, USA. Tel: +1-415-502-7211; fax: +1-415-476-5229.

E-mail addresses: djpappas75@gmail.com (D. J. Pappas), gabattop@anesthesia.ucsf.edu (P. A. Gabatto), doksenberg@gmail.com (D. Oksenberg), kpouya@gmail.com (P. Khankhanian), sebaran@cgl.ucsf.edu (S. E. Baranzini), lgan@gladstone.ucsf.edu (L. Gan), jorge.oksenberg@ucsf.edu (J. R. Oksenberg).

Abbreviations: CBP, cAMP-response element binding protein; CREB, c-AMP response element binding protein; DEG, differentially expressed genes; DKS, domain knowledge scores; HIF, hypoxic inducible factor; IFN, interferon; IRF7, interferon regulatory factor 7; MAPK, mitogen-activated protein kinase; MCAO, middle cerebral artery occlusion; MEF-2, myocyte enhancer factor 2; NMDA, *N*-methyl-D-aspartate; NMDA-R, NMDA receptors; TF, transcription factors; TFBS, TF binding sites; TLR, Toll-like receptor; TRAF4, TNF receptor-associated factor 4.

0306-4522/12 $36.00
http://dx.doi.org/10.1016/j.neuroscience.2012.09.007

pore potassium channel agonist (Mathie and Veale, 2007). Also, the standard model has been limited by a neuronal centric view. However, astrocytes and oligodendrocytes are critical players in glutamate regulation and express a similar complement of ionotropic and metabotropic glutamate receptors that render them vulnerable to excitotoxic injury (Bolton and Paul, 2006).

Finally, while many pathogenic mechanisms of glutamate excitotoxicity and cell death pathways have been well established, we still do not fully understand the complexities and multiplicity of networks, pathways, and intracellular signaling cascades that promote neuroprotection and cell survival (Lau and Tymianski, 2010). To increase our understanding of the intracellular mechanisms of neuroprotection, the current study used genome-wide expression analysis followed by a multi-step analytical approach that included text and database mining, as well as biological systems analysis. By employing primary mouse cortical neurons exposed to an excitotoxic insult of NMDA in the presence or absence of neuroprotective molecules, we were able to identify expression profiles that may represent shared signatures of neuroprotection. Interestingly, while diverging chemically and acting through different putative mechanisms of action, we found that these molecules converged at the level of whole-genome transcription. Namely, these signatures include mitogen-activated protein kinase (MAPK) signaling, calcium ion transport, and cellular adhesion, as well as pathways related to ischemic tolerance, such as the hypoxic inducible factor (HIF) and Toll-like receptor (TLR) pathways. Activation of these pathways may underlie a fundamental mechanism driving neuronal survival.

EXPERIMENTAL PROCEDURES

Primary cortical neuron generation

Generation of cortical neurons from postnatal day-0 CD-1 mice brains (Charles River Laboratories, Wilmington, MA, USA) was achieved by papain (Worthington Biochemical Corporation, Lakewood, NJ, USA, LS003126) dissociation and manual trituration (Chen et al., 2005). Dissociated cells (6×10^5 cells/ml) were cultured on poly-ornithine/poly-lysine (Sigma, St. Louis, MO, USA, P3655, P5282)-coated 10-cm plates in neurobasal A medium (NBA) (Invitrogen, Grand Island, NY, USA, 10888-022) supplemented with B-27 (Invitrogen, 17504-044) and penicillin/streptomycin (Invitrogen, 15140-122). Neurons were cultured for 7 days at which time the NBAM was replaced and all molecule testing and treatment was performed. All experimentation was carried out in accordance with the National Institute of Health Guide for the Care and Use of Laboratory Animals (NIH Publications No. 80-23) and received the approval of the UCSF Institutional Animal Care and Use Committee (IACUC). Formal approval can be provided upon request. All efforts were made to minimize the number of animals used and their suffering.

Neuroprotection assays

Neuroprotection was assessed using the Cell-Titer Glo® Luminescent Cell Viability Assay (Promega, Fitchburg, WI, USA, G7571) according to the manufacturer's protocol. Initially, each molecule was titrated over a twofold dilution curve (eight technical replicates were concentration) to determine neuroprotective efficacy following a NMDA-induced excitotoxic shock. Molecule concentrations that resulted in the highest level of cell viability (Table 1) were used for subsequent RNA extraction and microarray analysis. Of the 20 molecules used, 14 were classified as protective and six non-protective. The experimental design included single replicates for treatments with the 20 molecules and five biological replicates for non-treatment/vehicle controls. For RNA isolation, culture neurons were pre-treated for 1 h in NBAM+ media (NBAM with either media alone, vehicle, or molecule), followed by a 1-h incubation in excitotoxic media (EXM+, 120 mM NaCl, 5.3 mM KCL, 1.8 mM $CaCl_2$, 15 mM D-glucose, 25 mM Tris, pH 7.4 supplemented with 10 μM glycine and 100 μM NMDA) containing the respective molecule additives as in the NBAM+. Following incubation, neurons were washed with NBAM, and incubated for an additional 16 h in the respective NBAM+, at which time the cells were harvested for RNA isolation (see below).

RNA isolation, microarray analysis, and quantitative RT-PCR

Total RNA was extracted using the RNeasy Mini Kit (Qiagen, Valencia, CA, USA, 74104) according to the manufacturer's recommended protocols. For microarray analysis, 4 μg of total RNA was sent to the Keck Foundation Biotechnology Resource at Yale University (New Haven, CT, USA) and assayed using the MouseWG-6 v1.1 Expression Bead Chips (Illumina, San Diego, CA, USA). The data were deposited in the National Center for Biotechnology Information Gene Expression Omnibus (Barrett et al., 2011), GEO ID: GSE38701. RNA expression from single genes was assessed using TaqMan® Gene Expression assays (Applied Biosystems, Carlsbad, CA, USA, 4440040) on an ABI 7900HT Sequence Detection System, following all manufacturers' protocols. Assays were performed in triplicate using ~50 ng of RNA per reaction and reported using the $\Delta\Delta C_t$ comparative method as detailed in the ABI User Bulletin #2, using *Gapdh* as the sample calibrator and the references (relative controls) indicated in respective figures.

Neuronal transfection and RNA interference

For functional assays following *Irf7* interference, CD-1 mouse cortical neurons (Lonza, Basel, Switzerland, M-Cx-400) were cultured according to the manufacturer's protocol. Approximately 5×10^5 cells/well were cultured on 24-well poly-ornithine/poly-lysine-coated plates. On Day 7 post-plating, the medium was replaced with 50% fresh medium and the neurons were transfected with *Silencer*® siRNA oligos (Ambion, Carlsbad, CA, USA, 4390771) or mock (vehicle) using the GeneSilencer siRNA Transfection Reagent (Genlantis, San Diego, CA, USA, T500020) according to manufacturer's protocol. On Day 8, 24 h following transfection, neurons were subjected to the pretreatment/excitotoxic stimulus as detailed above (''Neuroprotection Assays'') and to a 16-h recovery period, at which time RNA was isolated or survival was quantitated. Transfection efficiency was assessed using the pmaxGFP® vector (Lonza, VSC-1001).

Data and statistical analysis

Expression data were background subtracted and normalized using cubic splines in the Illumina BeadStudio Gene Expression module v3.1. Illumina probes were annotated using version 4 of the Illumina whole-genome array annotation file, with occasional manual annotation using GeneAnnot (Chalifa-Caspi et al., 2004) and the Mouse Genome Institute database (Blake et al., 2010). Differentially expressed genes (DEG)

Table 1. Molecules used in neuroprotective studies

Molecule	Source[a]	Mechanism of action	Array	[Conc.]	Survival ratio[b]	Class[c]
Citicoline	S, C0256-500MG	Free radical scavenger	CIT	400 μM	0.81	NP
Flecainide	S, F6777-100MG	Ion channel blocker	FLE	25 μM	0.91	NP
Indomethacin	C, 405268	Enzyme inhibitor	IDO	800 nM	1.41	P
4-PPBP	B, NO104-0010	Receptor agonist	4 PB	5 μM	0.89	NP
Cyclophosphamide	C, 239785	Immunomodulator	CYC	40 μM	1.68	P
Ifenprodil	S, I2892-25MG	NMDAR antagonist	IFD	5 μM	1.81	P
Resveratrol	C, 554325	Enzyme inhibitor	RES	5 μM	1.55	P
Agmatine	S, A7127-1G	Receptor agonist	AGM	100 μM	0.61	NP
MK-801	C, 475878	NMDAR antagonist	MK8	10 μM	1.41	P
Riluzole	C, 557324	NMDAR antagonist	RIL	40 μM	1.88	P
Moxalactam	S, M8158-1G	Antibiotic	MOX	12.5 μM	1.80	P
Rolipram	C, 557330	Enzyme inhibitor	ROL	50 μM	2.77	P
Baclofen	S, B5399-5G	Receptor agonist	BAC	4 μM	0.97	NP
Liothyronine	S, T2877-500MG	Hormone	LIO	1 μM	1.56	P
Methotrexate	C, 454125	Enzyme inhibitor	MTX	160 μM	1.62	P
Benzamide	C, 165350	Enzyme inhibitor	BEN	16 μM	2.02	P
EthylFerulate	B, FR116-0100	Enzyme inhibitor	ETF	25 μM	0.99	NP
Memantine	S, M9292-100MG	NMDAR antagonist	MEM	80 μM	1.45	P
Necrostatin-1	B, AP309-0020	Antiapoptotic	NEC	250 nM	1.63	P
Carbenoxolone	S, C4790-1G	Enzyme inhibitor	CAR	12.5 μM	1.51	P

[a] B, Biomol, Farmingdale, NY, USA; C, CalBioChem, Darmstadt, Germany; CS, Cell Sciences, Canton, MA, USA; S, Sigma, St. Louis, MO, USA.
[b] Ratio relative to negative control in cytotoxicity assay.
[c] NP = not-protective; P = protective.

between protective and non-protective molecule classes were identified using the Microsoft Excel add-in BRB Array Tools (Dr. Richard Simon and BRB-ArrayTools Development Team) class comparison tool (*t*-test), controlling for the proportion of false discoveries (FDR p-value $\leqslant 0.2$). We applied thresholds and removed genes based on (1) significance relative to vehicle in a class comparison (controls with and without vehicle), (2) genes that did not show at least 20% difference in expression between the protective and non-protective class average expression, and (3) failure to achieve significance in a non-parametric Wilcoxon rank sum test (FDR p-value $\leqslant 0.2$). We performed hierarchical clustering (Manhattan Distance) with the Multiple Experiment Viewer, MeV (Saeed et al., 2003). Cytoscape (Shannon et al., 2003) was used for network visualization and image creation. Graphs and tables were created using Microsoft Excel. Statistical significance for differences in mRNA expression by quantitative PCR and survival from the cytotoxicity assays were assessed using a *t*-test. Statistically significant differences of domain knowledge scores (see below) differences was determined using a fisher's exact test and of simple parameters from the NetworkAnalyzer Cytoscape plug-in output (see below) using a binomial test. The level of significance for each test was set at a p-value $\leqslant 0.05$, unless otherwise indicated.

Significant enrichments of biological labels including functional ontology annotations, pathways, and transcription factor binding sites were performed using the Web-based Gene set Analysis tool (WebGestalt), functional analysis tool (Zhang et al., 2005) and the promoter analysis interaction tool (PAINT) (Vadigepalli et al., 2003).

Domain knowledge score

Domain knowledge scores for a list of genes were calculated using a text mining strategy as previously described (Baranzini et al., 2010). Briefly, an automated PubMed search was performed on each gene from the list in conjunction with (AND) the search phrase "('neuroprotection' OR 'neuroprotective' OR 'neuronal survival')." PubMed results for each gene were capped at 10 to control for bias due to extremes in molecule characterization or homographs of the molecule search term. The domain knowledge score was defined as the number of genes with $\geqslant 3$ reported results across all genes in the list.

Biological systems analysis

The integrated complex trait networks (iCTNet) Cytoscape plug-in (Wang et al., 2011a) retrieves data from several sources to form integrated networks that can contain genes (proteins), tissues, phenotypes (diseases and traits), and drugs. The accessed databases included the Human Protein Reference Database (HPRD) (Peri et al., 2003), the UCSC genome browser v.18 (Kent et al., 2002); the GWAS catalog (January 2011) (Hindorff et al., 2009), (restricted to strong associations, $p < 10^{-8}$); protein–drug associations, DrugBank v.2.5 (Wishart et al., 2008). The resulting 'initial network' (INTnet) consisted of 11,188 nodes (26 tissues, 9065 genes, 1863 drugs, and 234 phenotypes) that were connected by 70,399 edges. The overlapping DEG within the INTnet were mapped and extracted (genes/proteins only, including adjacent edges) to establish a core network of differentially expressed interacting nodes. The 20% class difference threshold for DEG identification was relaxed to increase the number of overlapping and interconnected genes resulting in a network of 357 nodes and 80 edges. This core network of differentially expressed genes was termed the DEGnet. The Cytoscape plug-in NetworkAnalyzer (Assenov et al., 2008) was used to compute basic topological parameters of each network and to compare these values to ten randomly generated networks of identical size (357 nodes) derived from the list of all genes in the network (9065). First-degree node neighbors (diseases and drugs) from the INTnet were added into the DEGnet, to form an integrated network of DEGs, diseases and drugs, called the (D3net).

RESULTS

Transcriptome overview

The transcriptional events associated with neuroprotection following glutamate excitotoxicity in mice cortical neuron primary cultures were measured

using microarray technology. Our experimental strategy consisted of culturing primary murine neurons that were subjected to glutamate receptor-induced excitotoxicity using NMDA in the presence or absence of a neuroprotective agent. To allow comparisons based on biological pathways and network analyses, we first identified DEG transcripts. Anticipating that moderately neuroprotective molecules would dilute the expression variance in a class comparison, we chose to analyze the most extreme phenotypes based on the neuroprotective ratios in the viability assay (Table 1). Based on this assay we defined two phenotypic classes: non-protective (viability ratios $\leqslant 1$) and protective (viability ratios $\geqslant 1.4$). Class comparisons and subsequent filtering (see Experimental procedures) identified 746 DEGs. Relative to the mean expression across the arrays, the hierarchical clustering demonstrates that neuroprotective molecules were associated with elevated expression of 368 transcripts (lower-right quadrant, high expression group, HighEG) and reduced expression of 378 transcripts (upper-right quadrant, low expression group, LowEG) (Fig. 1a).

To determine the biological relevance of the DEG signatures, we first employed a text mining strategy to calculate their respective domain knowledge scores, DKS (Baranzini et al., 2010). We computed the DKS for the full list of DEG and each of the HighEG and LowEG groups and compared them to that for all genes on the chip. We found that the DKS of each list was significantly higher ($p < 10^{-6}$, Welch's *t*-test) than the background of all genes on the Illumina MouseWG-6 v1.1 chip (Fig. 1b), supporting the biological relevance of these signatures in regard to neuroprotection or neuronal survival.

Enriched biological labels

The transcriptional patterns underlying neuroprotection could be classified according to known biological categories, such as gene ontologies, KEGG pathways, and transcriptional regulatory elements. We used WebGestalt (Zhang et al., 2005) to search for and contrast unique over-represented biological categories (adjusted $p \leqslant 0.01$) within the DEG, HighEG, and LowEG.

Gene ontology. The neuroprotective LowEG was enriched (adjusted $p \leqslant 0.01$) for biological processes related to DNA metabolic processes, as well as complementary enrichments for cellular compartments in the nucleus and chromosomal regions (Table 2). Contrastingly, the neuroprotective HighEG was uniquely enriched (adjusted $p \leqslant 0.01$) in transcripts involved in ion/nucleic acid transport, synaptic transmission/transport, and neuronal development (Table 2). This group of transcripts was also enriched in components of axonal and synaptic cellular compartments, as well as for molecular functions relating to ion channel activity and nucleic acid transport. Thus, the ontological analysis clearly highlighted mechanistic differences between transcripts that correlated with either neuronal loss or survival.

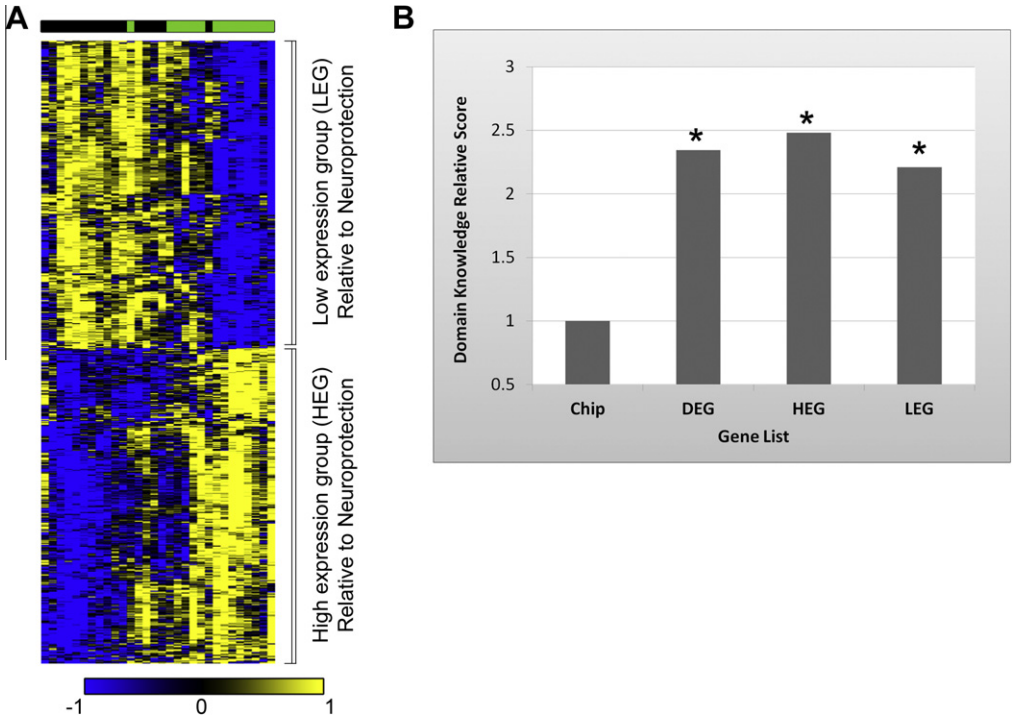

Fig. 1. Differentially expressed genes. (A) Hierarchical clustering, Euclidean distance metric. Each row (transcript) was normalized by subtracting the respective row mean and dividing by the row standard deviation. High and low expression groups, HighEG and LowEG, respectively, are indicated along the right side. Top shaded bar indicates protective class: green, neuroprotective; black, non-neuroprotective. Refer to Table 1 for the list of molecules. Transcripts shaded according to the bottom shaded bar ($\log_2$ scale). (B) Domain knowledge score. Relative score (to the DKS of the array chip) of each gene list was significantly higher than those of the background chip (*$p < 10^{-6}$, Welch's *t*-test).

Table 2. Ontology enrichment

Group	Category	Ontology[a]	Representative genes
HighEG	BP	Neurotransmitter transport	*Grik5*, *Nf1*, *Nrxn1*, *Nrxn3*, *Slc32a1*, *Slc6a11*, *Slc6a6*, *Sv2a*, *Syt1*
	BP	Dendrite development	*Bbs4*, *Cdk5*, *Dcx*, *Dscam*, *Mtap1b*, *Ppp1r9b*
	BP	Negative regulation of nucleocytoplasmic transport	*Cdk5*, *Nf1*, *Pkia*
	BP	Vesicle fusion	*Grik5*, *Pldn*, *Snph*
	BP	Regulation of postsynaptic membrane potential	*Cdk5*, *Foxp2*, *Gphn*, *Homer1*, *Myl6b*, *Nf1*, *Ppp3ca*
	BP	Regulation of synaptic transmission	*Cdk5*, *Grik5*, *Grik1*, *Ppp3ca*
	CC	Synapse	*Ank3*, *Cadps*, *Gphn*, *Grik1*, *Grik5*, *Homer1*, *Magee1*, *Nlgn2*, *Nrxn1*, *Nrxn3*, *Ophn1*, *Pja2*, *Ppp1r9b*, *Sept3*, *Slc32a1*, *Snph*, *Sv2a*, *Syt1*, *Znrf1*
	CC	Axon	*Ank3*, *Cdk5*, *Cntn2*, *Klc1*, *Mapk8ip3*, *Mapt*, *Tubb4*
	MF	Calcium channel regulator activity	*Nrxn1*, *Nrxn3*, *Prkcb*
	MF	Solute:sodium symporter activity	*Slc32a1*, *Slc28a3*, *Slc6a6*, *Slc6a11*, *Slc1a1*
LowEG	BP	DNA metabolic process	*1110054O05Rik*, *Cdc45l*, *Cdt1*, *Ercc1*, *Fanci*, *Gins2*, *Kif22*, *Mcm10*, *Mre11a*, *Mutyh*, *Parp1*, *Rad51ap1*, *Rad9*, *Rbbp7*, *Rfc2*, *Rfc3*, *Rpa2*
	CC	Chromosome	*Cdca8*, *Cenpi*, *Cenpl*, *Cenpm*, *Fanci*, *Hist1h2af*, *Kif22*, *Oip5*, *Pbrm1*, *Rfc2*, *Rpa2*, *Smc2*, *Tmpo*, *Wapal*
	MF	Carbohydrate kinase activity	*Khk*, *Nagk*, *Pfkp*, *Rbks*
	MF	Iron–sulfur cluster binding	*Aifm3*, *Mutyh*, *Nubp2*, *Rsad2*
	MF	Heparin binding	*App*, *Fn1*, *Fstl1*, *Hbegf*, *Hdgf*

[a] Top adjusted *p*-values $\leqslant 0.01$, ratios of enrichment $\geqslant 3$, and higher GO level are shown.

KEGG pathways. We also found unique KEGG pathway enrichments (adjusted $p \leqslant 0.01$) between the LowEG and HighEG (Table 3). Specifically, the LowEG was enriched for nucleic acid excision repair, DNA replication, focal adhesion, extracellular matrix receptor (ECM) interactions, mismatch repair, and metabolic pathways. The nucleic acid repair and replication pathways overlapped in three repair genes (*Rfc3*, *Rfc2*, *Rpa2*), while the adhesion pathways overlapped in three extracellular matrix genes (*Itgb5*, *Fn1*, *Col4a6*). The HighEG was enriched for components of MAPK signaling, gap and tight junctions, and cell adhesion pathways. The MAPK signaling pathway included genes from the ERK1/2 (*Rasgrp1*, *Prkcb*, *Pdgfrb*) and JNK (*Map2k4*, *Mapk10*, *Jun*) branches.

Transcription factor binding sites. Stimulation of transcriptional changes requires the activation of transcription factors (TF) and the engagement of regulatory elements. We searched for enrichment of TF binding sites (TFBS) within the 5000-bp upstream promoter regions of the DEGs. We identified a common core of significantly enriched TFBS (Table 4) by taking the intersection (adjusted $p < 0.01$) between two analysis tools, WebGestalt (Wang et al., 2011b) and PAINT (Vadigepalli et al., 2003). Both analyses detected TFBS in the HighEG previously linked to general neuroprotection, as well as neuroprotection through the establishment of ischemic tolerance such as Arnt (HIF-1β), CREB, SRF, ER-alpha and Cart-1 (TRAF4) (Gidday, 2006, 2010). WebGestalt also identified

Table 3. KEGG pathway enrichment

Group	Enriched pathways[a]	Genes
HighEG	MAPK signaling pathway	*Dusp8*, *Cacng5*, *Mapk10*, *Prkcb*, *Map2k4*, *Mapk8ip3*, *Nf1*, *Pdgfrb*, *Rasgrp1*, *Ppp3ca*, *Mapt*
	Gap junction	*Adcy6*, *Tubb4a*, *Pdgfrb*, *Prkcb*, *Gnai1*, *Adcy9*
	Cell adhesion molecules	*Nrxn1*, *Pvrl3*, *Nlgn2*, *Pvrl1*, *Nrxn3*, *Cntn2*
	Tight junction	*Pard6a*, *Ppp2r2b*, *Spnb2*, *Magi1*, *Prkcb*, *Gnai1*
	GnRH signaling pathway	*Adcy6*, *Mapk10*, *Prkcb*, *Map2k4*, *Adcy9*
LowEG	Nucleotide excision repair	*Rfc3*, *Ercc1*, *Rfc2*, *Rpa2*, *Mnat1*
	DNA replication	*Rfc3*, *Rfc2*, *Rpa2*, *Rnaseh2c*
	Mismatch repair	*Rfc3*, *Rfc2*, *Rpa2*
	Focal adhesion	*Flnc*, *Itgb5*, *Fn1*, *Pxn*, *Col4a6*, *Cav2*
	ECM-receptor interaction	*Cd44*, *Itgb5*, *Fn1*, *Col4a6*
	Metabolic pathways	*Pet112l*, *Acsl5*, *Dhrs4*, *Hdc*, *Khk*, *Qars*, *Smpd4*, *Nme5*, *Gch1*, *Ppap2c*, *Pfkp*, *Ak7*, *Upp1*, *mt-Nd6*

[a] WebGestalt, adjusted *p*-values < 0.001.

Table 4. Transcription factor binding sites enrichment

Transcription factor binding site[a,b]	Group
HIF-1β (*Arnt*)	HighEG
Cart-1 (*Traf4*)	HighEG
CUTL1 (*Cux1*)	HighEG
CREB (*TAXCREB*)	HighEG
E4BP4 (*Nfil3*)	HighEG
ER-alpha (*Esr1*)	HighEG
Evi-1 (*Mecom*)	HighEG
GATA-2 (*Gata2*)	HighEG
GR-alpha (*Nr3c1*)	HighEG
MEF-2 (*Mef2*)	HighEG
Myogenin:**NF-1** (*Myog*:***Nf1***)	**HighEG**
Oct-1 (*Pou2f1*)	**HighEG**
Rfx1	HighEG
Stat1	HighEG
Tgif1	HighEG
ZID (*Zbtb6*)	HighEG
Irf-2 *(Irf2*)	LowEG

[a] FDR *p*-value < 0.01. WebGestalt and PAINT overlaps.
[b] Bold, DEG. Parenthetical/italic, official gene name.

significant enrichment of factors from the interferon enhanceosome including interferon regulatory factor 7 (IRF7), HMGI(Y), ATF-2, NF-κB, cJun, and cAMP-response element binding protein (CBP)/p300 (data not shown) in the HighEG. Both analysis tools overlapped in the identification of IRF2 in the LowEG.

From the common core of enriched TFBS, the POU class 2 homeobox 1 (*Pou2f1*, a.k.a. *Oct1*) and neurofibromin 1 (*Nf1*) (both from the HighEG) were found to be differentially regulated between neuroprotective classes.

Transcription factor targeting

The connection to TLR pathways described above prompted us to investigate the role of IRF7 and type-I interferons in neuronal survival. Interestingly, *Irf7* expression was up-regulated and IRF7 TFBS were enriched following acute demyelination (Schmidt et al., 2009), viral infection (Ousman et al., 2005), and middle cerebral artery occlusion (Stevens et al., 2011). We then measured *Irf7* expression in cultures of cortical neurons pre- and post-excitotoxic stimulus and found that *Irf7* expression was up-regulated following NMDA treatment (Fig. 2, PreStimulus versus PostStimulus), suggesting that it may also be involved in responses to glutamate receptor-induced excitotoxic injury. We then tested if gene silencing of *Irf7* using RNA interference (RNAi) would affect neuronal survival. Transfection with *Irf7* siRNA oligonucleotides resulted in more than a 40% ($p < 0.03$) repression of this stimulation relative to control transfection with mock or negative control oligonucleotides (Fig. 2, PostStimulus-mock versus PostStimulus-*Irf7*). In contrast semaphorin-3a (*Sema3a*), a control gene not present in the DEG list or known to be an IRF7 target, did not evidence significant changes in its expression following either the excitotoxic stimulus or siRNA transfection (Fig. 2). We then measured how reduction of *Irf7* expression affected neuronal survival. We observed that the downregulation of *Irf7* expression was concomitant with a modest but significant reduction (15%, $p < 10^{-6}$) in neuronal survival (Fig. 3a) relative to controls. The modest effect we observed may be a result of lower transfection efficiency (see Experimental procedures), the remaining IRF7 message, and redundancy in pathways that promote neuronal survival. Given the importance that IRF7 plays in the regulation of type-I interferon (IFN) expression, we also tested whether type-I interferons, interferon-α2 (IFN-α2) and interferon-β (IFN-β), could themselves serve as neuroprotective molecules. We found that both IFN-α2 and IFN-β enhanced neuronal survival relative to untreated control (Fig. 3b). In summary, these data are consistent with a model where *Irf7* up-regulation, following neuronal insult, maximizes neuronal survival through stimulation of type-I interferons.

Integrated complex trait networks

To identify modules of interacting genes, we used the integrated complex trait network (iCTnet) Cytoscape plug-in (Wang et al., 2011a). We captured all associations from the protein–protein interactome, whole genome association studies, and drug–target

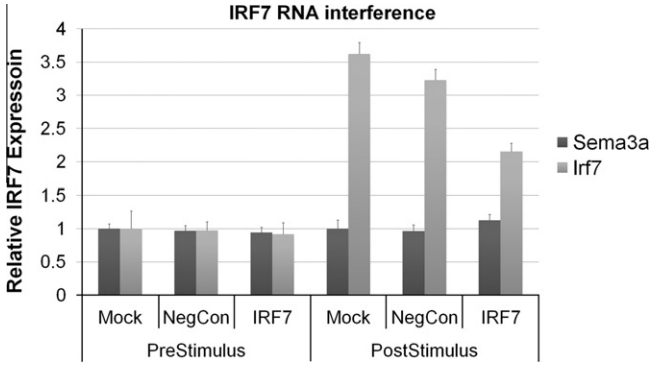

Fig. 2. IRF7 expression following excitotoxicity and RNAi. *Irf7* and *Sema3a* expression in neuronal samples either before NMDA excitotoxic stimulus (Pre) or after stimulus and a 16-h recovery period (Post). Neurons were transfected 24 h prior to excitotoxic stimulus with either Mock (vehicle), negative control siRNA (NegCon), or I*rf7*-specific siRNA oligo. qRT-PCR $\Delta\Delta C_t$ quantitation method: calibrator, GAPDH; reference, pre-assay mock.

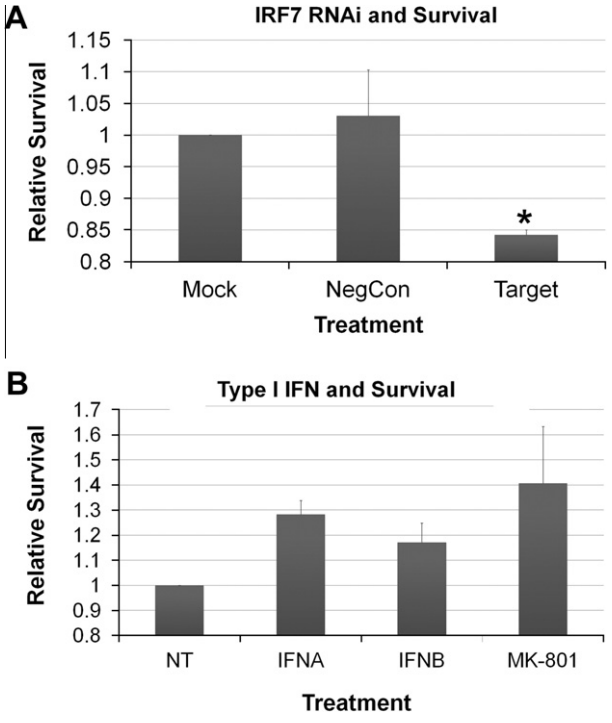

Fig. 3. Survival effects of IRF7 RNAi and Type-I Interferons. (A) Neuronal survival following *Irf7* RNAi. Survival assay following 16-h recovery period for transfected neurons. $N = 3$. $^{*}p < 10^{-6}$ (Student's *t*-test). Neurons were transfected 24 h prior to excitotoxic stimulus with either Mock (vehicle), negative control siRNA (NegCon), or I*rf7*-specific siRNA oligo. (B) Survival assay (see Experimental procedures) in the presence of type-I IFNs (left to right) NT = vehicle control, IFNA = IFN-α, IFNB = IFN-β ($N = 4$), MK-801, positive control NMDA receptor anatagonist.

interactions (see Experimental procedures), combining all available information into a large integrated network (INTnet, not shown) onto which we mapped our differentially expressed genes. At the protein level, the overlapping nodes and their adjacent edges were extracted, resulting in a core network of differentially expressed genes (DEGnet, not shown). The DEGnet consisted of 357 nodes and 80 edges that were comprised of several smaller subnetwork clusters or modules. To test if the resultant modules and overall topology within the DEGnet could be the result of random sampling, we compared DEGnet topological parameters from the Cytoscape plug-in NetworkAnalyzer (Assenov et al., 2008) to 10 randomly generated networks of equal size. We found that our DEGnet differed significantly ($p < 0.001$, binomial test) across a wide spectrum of parameters relative to randomly generated networks, including the greatest number of edges, the largest connected cluster, the most connected pairs, and the largest node density (Table 5). These findings strongly suggest the identified transcripts are functionally related.

We then incorporated any disease and drug having direct links to the core nodes within the INTnet, thus creating a larger network of interconnected DEGs, diseases, and drugs (D3net, Fig. 4). From the initial 234 diseases that were present in the INTnet, we found that our D3net nodes were exclusively connected to CNS and inflammatory disorders such as Parkinson's disease, Alzheimer's disease and Rheumatoid Arthritis. We focused on D3net modules consisting of at least five or more genes. The largest, a cluster of 47 genes, was built upon a backbone of four highly connected genes, including *Cdk5*, *Mapk10*, *Jun*, *Smad3*, *Dcx*, *Trim39*, and *Ptpn11*. The other three consisted of smaller connected modules of nine and seven genes, including the more connected genes, *Cd44*, *Ee4f1a1*, and *Homer1*. We applied the DKS algorithm to assess literature support for each module within the DEGnet and found that modules 7-1 and 7-2 showed a significantly higher DKS than the DEGnet as a whole (Fig. 4 inset, $p < 0.03$, Welch's *t*-test). Module 7-1 was found to be a mixture of glutamate receptors (*Gria*, *Grik*), a glutamate transporter (*Slc1a1*) and glutamate receptor scaffolding gene (*Homer1*). Whereas module 7-2, was composed exclusively of molecules involved in extracellular matrix assembly such as fibronectin 1 (*Fn1*), collagen type IV alpha 6 (*Col4a6*), and the heparin sulfate proteoglycan, *Cd44*.

DISCUSSION

The panel of molecules used to promote neuronal survival included such mechanistic diversity as ion channel blockers, enzyme inhibitors, cytokines, free radical scavengers, α/β-adrenergic antagonists, and NMDA-R antagonists. Our analysis demonstrated that the molecular diversity, rather than translating into divergent mechanisms of neuroprotection, converged on the regulation of key genes and pathways of neuronal survival. These players fell into a few major themes that included the regulation of ion channels and co-transporters, the regulation of signaling pathways including the MAPK pathway, the HIF pathway, and the TLR signaling pathway, the regulation of cellular adhesion, and the regulation of nucleic acid metabolism and repair.

Neuroprotection from ischemia and excitatory amino acids has been shown to involve the activation of ion channels and transporters, including glutamate receptors that reside in pre- and post-synaptic membranes (Besancon et al., 2008; Hardingham and Bading, 2010). From the ontological analysis, we found enhanced expression of solute carriers for sodium ions, including the Na(+)-dependent glutamate transporter (*Slc1a1*, previously *Eaat3*), which was important for neuroprotection through preconditioning for middle cerebral artery occlusion (MCAO) in rat brains (Romera et al., 2004). Moreover, we identified elevated expression of a network module with a high domain knowledge score, or literature support, for neuroprotection. This module consisted of the AMPA (*Gria1*) and kainite (*Grik1*, *Grik5*)-type glutamate receptors, *Slc1a1*, and the scaffolding protein *Homer1*. Genes whose resultant proteins are generally localized to synaptic membranes and whose activation, in the case of kainite-type receptors, may promote growth and remodeling (Lau and Tymianski, 2010). Estrogen

Table 5. DEGnet and random network topological parameters

Network topological parameters	DEGnet	Average of 10 random nets	*p*-value[a], binomial test
Nodes	357	357	n.t.
Edges	80	45	< 0.001
Largest cluster	35	12	< 0.001
Clustering coefficient	0.0052	0.0044	n.s.
Connected components	281	313	< 0.001
Diameter	9	5	< 0.001
Centralization	0.021	0.015	< 0.01
Connected pairs	1386	297	< 0.001
Shortest paths	4.0	2.2	< 0.001
Average number of neighbors	0.45	0.25	< 0.001
Density	0.0012	0.00071	< 0.001
Heterogeneity	2.11	2.631	< 0.001
Isolated nodes	259	293	< 0.001
Degree distribution	9	6.7	< 0.01

[a] n.t., not tested; n.s., not significant.

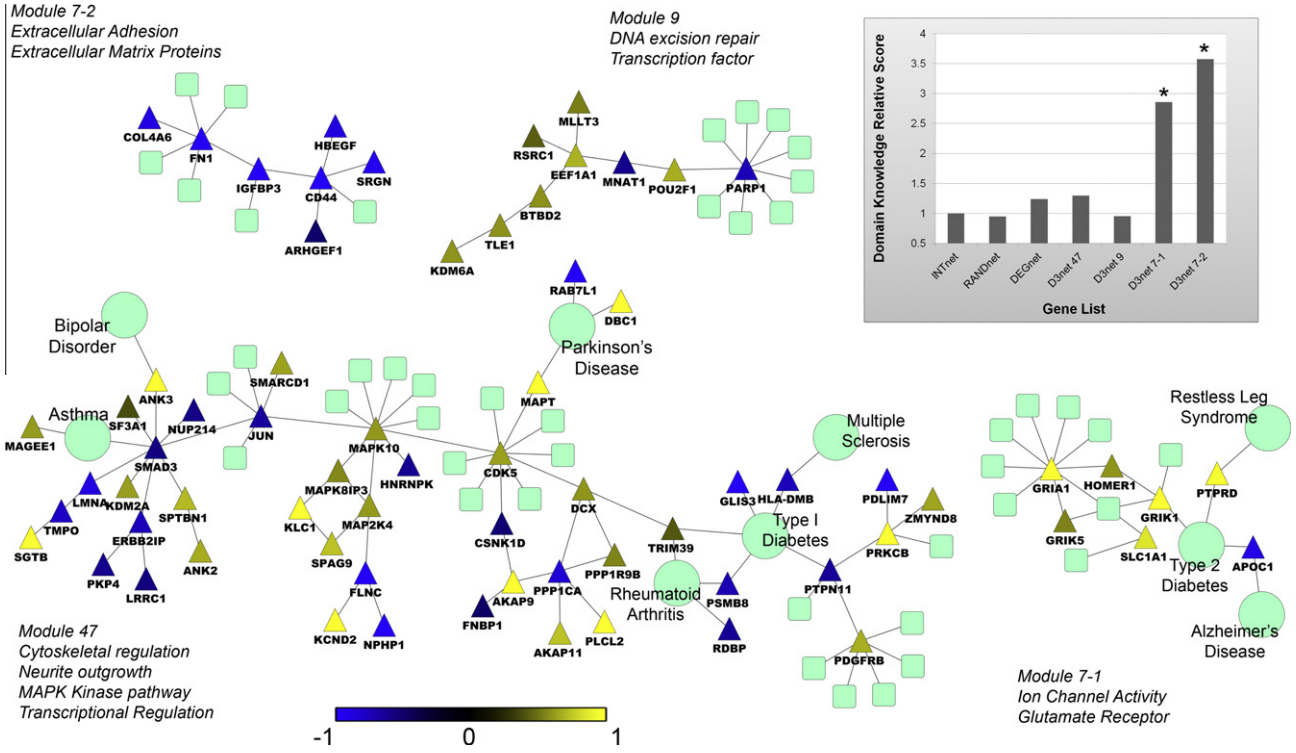

Fig. 4. Integrated differentially expressed gene network, D3net. Differentially expressed gene network (DEGnet) plus first-degree neighbor diseases (large cyan circles) and drugs (small cyan squares) from the integrated network (INTnet). DEG (triangles) coloring represents average transcript expression differences between protective and non-protective classes. Colored according to bottom bar, log2 scale. Module name and representative ontologies for each module. Inset graph: Relative (to INTnet) module DKS score. Modules 7-1 and 7-2 of each gene list was significantly higher than those of the background INTnet (*$p < 0.03$, Fisher's exact test). Only modules with four of more interconnected DEG shown.

neuroprotection from MCAO in rat brains required glutamate receptor activation and was attenuated by MK-801 (Connell et al., 2007). Estrogen has been thought to trigger the endoplasmic reticulum stress response (Ejima et al., 1999), a process that may be mediated by Homer1 (Connell et al., 2007). Similarly, excitotoxic neuroprotection against NMDA with resveratrol, a sirtuin-1 inhibitor, required the activation of both the estrogen and glutamate receptors (Saleh et al., 2009). These instances required the concomitant activation of the NMDA and estrogen receptors, either directly or indirectly. We also found that along with enhanced expression of glutamate receptors, neuroprotection across multiple compounds correlated with an enrichment of ER-alpha transcription factor signatures, perhaps indicative of their activation.

Stimulation of glutamate receptors, including NMDA, activates MAPK pathway components, specifically extracellular signal-regulated kinase 1/2 (ERK1/2) and c-Jun N-terminal kinase pathway (JNK) (Centeno et al.,

2007; Sawe et al., 2008). We found that across neuroprotective molecules, survival correlated with elevated expression of several key MAPK (ERK1/2) signaling pathway genes, including *Rasgrp1*, *Prkcb1* (protein kinase C, PKC), as well as several JNK signaling pathway genes, including *Mapk10* (JNK3) and *Map2k4* (MEK4). The biological systems analysis identified a large MAPK-containing module that included the low expression group JNK3 target, *Jun*. Preconditioning with sub lethal ischemia in rat models of tolerance required activation of NMDA-R and led to the phosphorylation of ERK1/2 (Jin et al., 2006; Zhang et al., 2009). Typically, the reduction of JNK3 activation supports increased neuroprotection (Yamasaki et al., 2012), for example in ethanol-attenuated neuronal injury following kainite treatment of rat brains (Qi et al., 2010). However, the reduction of c-Jun, may indicate reprogramming of the MAPK pathway, favoring ERK1/2 signaling or alternative targets of the MEK4/JNK3 pathway (Yamasaki et al., 2012).

We also identified enrichment for transcription factors known to be down-stream effectors of MAPK activation including the c-AMP response element binding protein (CREB), myocyte enhancer factor 2 (MEF-2), and TNF receptor-associated factor 4 (TRAF4). CREB activation is strongly induced by synaptic NMDAR activity (Hardingham, 2009) and both CREB (Hara et al., 2003; Terasaki et al., 2010) and MEF-2 (Wang et al., 2009) are protective against ischemia. TRAF4 a silencer of TLR signaling, was demonstrated to mediate TLR signaling through its association with TRAF6 and TRIF (Takeshita et al., 2005), as well as shown to regulate the JNK pathway through enhancement of MEKK4 activity (Abell and Johnson, 2005). Therefore, across multiple disparate neuroprotective molecules, the enhanced expression of both ERK1/2 and the JNK pathways may be important for long-term neuronal survival and stimulation of effectors such as CREB, MEF-2, and TRAF4.

Neuroprotection from hypoxia and activation of the hypoxic inducible factor 1 (HIF-1) are among the most well-studied examples of neuroprotection (Liu et al., 2009). We found that neuroprotection across the panel of molecules correlated with convergence on the HIF-1 pathway, including enrichments for signatures of the transcription factors HIF-1β and co-activator p300/CBP.

The TLR system plays an important role in sensing exogenous pathogens as well as endogenous stress molecules that occur in response to injury and has been established to be an important mechanism for neuroprotection and establishment of ischemic tolerance (Wang et al., 2011b). The identified TRAF4 had been previously found to be important for TLR silencing, pathway reprogramming (Takeshita et al., 2005), and downstream activation of IRF3/IRF7 (Stevens et al., 2011). IRF7 is an established critical regulator of type-I interferon expression and a component of the interferon enhanceosome (Honda et al., 2005). The transcription factor analysis identified enrichment not only for IRF7 transcription factor binding sites, but also other components of the IFN enhanceosome (Panne, 2008) including c-Jun, ATF-2, CBP, and NF-κB. We found that *Irf7* expression was up-regulated following the excitotoxic stimulus and *Irf7* RNA interference decreased gene expression and neuronal survival. IRF7 had been demonstrated to be an important regulator of type-I interferon (IFN) expression (Savitsky et al., 2010), as well as being an critical effector of preconditioning in a mouse model of tolerance (Marsh et al., 2009; Stevens et al., 2011). Moreover, mice deficient for either *Irf3* or *Irf7* have a significantly attenuated preconditioning response (Stevens et al., 2011). Given this, we tested if type I IFNs were neuroprotective. We found that either IFN-β or IFN-α alone was sufficient to enhance neuronal survival following NMDA exposure. The exacerbation of neuronal cell death following *Irf7* RNA interference may indicate that the IRF7-dependent transcription maximizes neuronal survival through the expression of type-I IFNs. This may represent the first description of type-I IFNs directly stimulating neuronal survival, rather than supporting survival through indirect immunomodulatory and anti-inflammatory mechanisms. The US Institute of Health's clinical trials registry (clinicaltrials.gov) has listed a National Institute of Neurological Disorders and Stroke funded phase I dose escalation trial for IFN-β1a in acute ischemia (NCT00097318) indicating interest in the application of type-I interferons in the prevention of stroke.

The biological systems analysis revealed the DEGs existed as small, interconnected modules that are more connected to themselves than would be expected by random chance, enhancing the biological relevance of the gene list and resultant network. These genes and module have been linked to neurologic, neurodegenerative, and inflammatory disorders. This remarkable finding suggests that, at the level of whole genome transcription, the same modules and genes important for ensuring neuroprotection also seem to be associated with disease pathology and recovery from injury. Strategies to protect neurons from excitotoxic injury and demyelination are challenges to current and future therapies. These will ultimately be necessary for effective treatment of neurodegenerative disorders where current approaches often mitigate disease symptoms and prolong disease course, albeit do not reverse prior damage, nor halt progression (Dong et al., 2009). Our study demonstrates that many exogenously delivered molecules with arguably different mechanisms of action, converged in their abilities to stimulate the genome.

One limitation of this study is that the transcriptional events observed were cross-sectional and represent long-term transcriptional changes. Given the dynamic nature of gene expression, capturing these transcriptional changes along a time series would be necessary to more comprehensively identify the molecular events leading to neuroprotection. Furthermore, extending this analysis to other key cell types (e.g., glial cells) would contribute to defining the transcriptional regulatory patterns involved in promoting overall neuronal survival. As our knowledge of neuroprotection increases, a combination of known

therapeutics or more rationally designed candidates may provide more stable, long-lasting, pharmacologically tractable neuroprotection.

Acknowledgments—We would like to thank Dr. Pierre-Antoine Gourraud for his intellectual contributions to the statistical analysis and Yungui Zhou for her technical assistance with the mouse dissection and cortical neuron isolation. This study was supported by grants from the National Institutes of Health (R01NS26799) and the National Multiple Sclerosis Society (RG2901).

REFERENCES

Abell AN, Johnson GL (2005) MEKK4 is an effector of the embryonic TRAF4 for JNK activation. J Biol Chem 280:35793–35796.

Assenov Y, Ramirez F, Schelhorn SE, Lengauer T, Albrecht M (2008) Computing topological parameters of biological networks. Bioinformatics 24:282–284.

Baranzini SE, Srinivasan R, Khankhanian P, Okuda DT, Nelson SJ, Matthews PM, Hauser SL, Oksenberg JR, Pelletier D (2010) Genetic variation influences glutamate concentrations in brains of patients with multiple sclerosis. Brain 133:2603–2611.

Barrett T, Troup DB, Wilhite SE, Ledoux P, Evangelista C, Kim IF, Tomashevsky M, Marshall KA, Phillippy KH, Sherman PM, Muertter RN, Holko M, Ayanbule O, Yefanov A, Soboleva A (2011) NCBI GEO: archive for functional genomics data sets – 10 years on. Nucleic Acids Res 39:D1005–D1010.

Besancon E, Guo S, Lok J, Tymianski M, Lo EH (2008) Beyond NMDA and AMPA glutamate receptors: emerging mechanisms for ionic imbalance and cell death in stroke. Trends Pharmacol Sci 29:268–275.

Blake JA, Bult CJ, Kadin JA, Richardson JE, Eppig JT (2010) The Mouse Genome Database (MGD): premier model organism resource for mammalian genomics and genetics. Nucleic Acids Res 39:D842–D848.

Bolton C, Paul C (2006) Glutamate receptors in neuroinflammatory demyelinating disease. Mediators Inflamm 2006:93684.

Centeno C, Repici M, Chatton JY, Riederer BM, Bonny C, Nicod P, Price M, Clarke PG, Papa S, Franzoso G, Borsello T (2007) Role of the JNK pathway in NMDA-mediated excitotoxicity of cortical neurons. Cell Death Differ 14:240–253.

Chalifa-Caspi V, Yanai I, Ophir R, Rosen N, Shmoish M, Benjamin-Rodrig H, Shklar M, Stein TI, Shmueli O, Safran M, Lancet D (2004) GeneAnnot: comprehensive two-way linking between oligonucleotide array probesets and GeneCards genes. Bioinformatics 20:1457–1458.

Chen J, Zhou Y, Mueller-Steiner S, Chen LF, Kwon H, Yi S, Mucke L, Gan L (2005) SIRT1 protects against microglia-dependent amyloid-beta toxicity through inhibiting NF-kappaB signaling. J Biol Chem 280:40364–40374.

Connell BJ, Crosby KM, Richard MJ, Mayne MB, Saleh TM (2007) Estrogen-mediated neuroprotection in the cortex may require NMDA receptor activation. Neuroscience 146:160–169.

Dong XX, Wang Y, Qin ZH (2009) Molecular mechanisms of excitotoxicity and their relevance to pathogenesis of neurodegenerative diseases. Acta Pharmacol Sin 30:379–387.

Ejima K, Nanri H, Araki M, Uchida K, Kashimura M, Ikeda M (1999) 17Beta-estradiol induces protein thiol/disulfide oxidoreductases and protects cultured bovine aortic endothelial cells from oxidative stress. Eur J Endocrinol 140:608–613.

Gidday JM (2006) Cerebral preconditioning and ischaemic tolerance. Nat Rev Neurosci 7:437–448.

Gidday JM (2010) Pharmacologic preconditioning: translating the promise. Transl Stroke Res 1:19–30.

Hara T, Hamada J, Yano S, Morioka M, Kai Y, Ushio Y (2003) CREB is required for acquisition of ischemic tolerance in gerbil hippocampal CA1 region. J Neurochem 86:805–814.

Hardingham GE (2009) Coupling of the NMDA receptor to neuroprotective and neurodestructive events. Biochem Soc Trans 37:1147–1160.

Hardingham GE, Bading H (2010) Synaptic versus extrasynaptic NMDA receptor signalling: implications for neurodegenerative disorders. Nat Rev Neurosci 11:682–696.

Hindorff LA, Sethupathy P, Junkins HA, Ramos EM, Mehta JP, Collins FS, Manolio TA (2009) Potential etiologic and functional implications of genome-wide association loci for human diseases and traits. Proc Natl Acad Sci USA 106:9362–9367.

Honda K, Yanai H, Negishi H, Asagiri M, Sato M, Mizutani T, Shimada N, Ohba Y, Takaoka A, Yoshida N, Taniguchi T (2005) IRF-7 is the master regulator of type-I interferon-dependent immune responses. Nature 434:772–777.

Hoyte L, Barber PA, Buchan AM, Hill MD (2004) The rise and fall of NMDA antagonists for ischemic stroke. Curr Mol Med 4:131–136.

Jin RL, Li WB, Li QJ, Zhang M, Xian XH, Sun XC, Zhao HG, Qi J (2006) The role of extracellular signal-regulated kinases in the neuroprotection of limb ischemic preconditioning. Neurosci Res 55:65–73.

Kent WJ, Sugnet CW, Furey TS, Roskin KM, Pringle TH, Zahler AM, Haussler D (2002) The human genome browser at UCSC. Genome Res 12:996–1006.

Lau A, Tymianski M (2010) Glutamate receptors, neurotoxicity and neurodegeneration. Pflugers Arch 460:525–542.

Liu XQ, Sheng R, Qin ZH (2009) The neuroprotective mechanism of brain ischemic preconditioning. Acta Pharmacol Sin 30:1071–1080.

Marsh B, Stevens SL, Packard AE, Gopalan B, Hunter B, Leung PY, Harrington CA, Stenzel-Poore MP (2009) Systemic lipopolysaccharide protects the brain from ischemic injury by reprogramming the response of the brain to stroke: critical role for IRF3. J Neurosci 29:9839–9849.

Mathie A, Veale EL (2007) Therapeutic potential of neuronal two-pore domain potassium-channel modulators. Curr Opin Investig Drugs 8:555–562.

Ousman SS, Wang J, Campbell IL (2005) Differential regulation of interferon regulatory factor (IRF)-7 and IRF-9 gene expression in the central nervous system during viral infection. J Virol 79:7514–7527.

Panne D (2008) The enhanceosome. Curr Opin Struct Biol 18:236–242.

Peri S, Navarro JD, Amanchy R, Kristiansen TZ, Jonnalagadda CK, Surendranath V, Niranjan V, Muthusamy B, Gandhi TK, Gronborg M, Ibarrola N, Deshpande N, Shanker K, Shivashankar HN, Rashmi BP, Ramya MA, Zhao Z, Chandrika KN, Padma N, Harsha HC, Yatish AJ, Kavitha MP, Menezes M, Choudhury DR, Suresh S, Ghosh N, Saravana R, Chandran S, Krishna S, Joy M, Anand SK, Madavan V, Joseph A, Wong GW, Schiemann WP, Constantinescu SN, Huang L, Khosravi-Far R, Steen H, Tewari M, Ghaffari S, Blobe GC, Dang CV, Garcia JG, Pevsner J, Jensen ON, Roepstorff P, Deshpande KS, Chinnaiyan AM, Hamosh A, Chakravarti A, Pandey A (2003) Development of human protein reference database as an initial platform for approaching systems biology in humans. Genome Res 13:2363–2371.

Qi SH, Liu Y, Hao LY, Guan QH, Gu YH, Zhang J, Yan H, Wang M, Zhang GY (2010) Neuroprotection of ethanol against ischemia/reperfusion-induced brain injury through decreasing c-Jun N-terminal kinase 3 (JNK3) activation by enhancing GABA release. Neuroscience 167:1125–1137.

Romera C, Hurtado O, Botella SH, Lizasoain I, Cardenas A, Fernandez-Tome P, Leza JC, Lorenzo P, Moro MA (2004) In vitro ischemic tolerance involves upregulation of glutamate transport partly mediated by the TACE/ADAM17-tumor necrosis factor-alpha pathway. J Neurosci 24:1350–1357.

Saeed AI, Sharov V, White J, Li J, Liang W, Bhagabati N, Braisted J, Klapa M, Currier T, Thiagarajan M, Sturn A, Snuffin M, Rezantsev A, Popov D, Ryltsov A, Kostukovich E, Borisovsky I, Liu Z, Vinsavich A, Trush V, Quackenbush J (2003) TM4: a free, open-source system for microarray data management and analysis. Biotechniques 34:374–378.

Saleh MC, Connell BJ, Saleh TM (2009) Resveratrol preconditioning induces cellular stress proteins and is mediated via NMDA and estrogen receptors. Neuroscience 166:445–454.

Savitsky D, Tamura T, Yanai H, Taniguchi T (2010) Regulation of immunity and oncogenesis by the IRF transcription factor family. Cancer Immunol Immunother 59:489–510.

Sawe N, Steinberg G, Zhao H (2008) Dual roles of the MAPK/ERK1/2 cell signaling pathway after stroke. J Neurosci Res 86:1659–1669.

Schmidt H, Raasch J, Merkler D, Klinker F, Krauss S, Bruck W, Prinz M (2009) Type I interferon receptor signalling is induced during demyelination while its function for myelin damage and repair is redundant. Exp Neurol 216:306–311.

Shannon P, Markiel A, Ozier O, Baliga NS, Wang JT, Ramage D, Amin N, Schwikowski B, Ideker T (2003) Cytoscape: a software environment for integrated models of biomolecular interaction networks. Genome Res 13:2498–2504.

Sheldon AL, Robinson MB (2007) The role of glutamate transporters in neurodegenerative diseases and potential opportunities for intervention. Neurochem Int 51:333–355.

Song JH, Huang CS, Nagata K, Yeh JZ, Narahashi T (1997) Differential action of riluzole on tetrodotoxin-sensitive and tetrodotoxin-resistant sodium channels. J Pharmacol Exp Ther 282:707–714.

Stevens SL, Leung PY, Vartanian KB, Gopalan B, Yang T, Simon RP, Stenzel-Poore MP (2011) Multiple preconditioning paradigms converge on interferon regulatory factor-dependent signaling to promote tolerance to ischemic brain injury. J Neurosci 31:8456–8463.

Takeshita F, Ishii KJ, Kobiyama K, Kojima Y, Coban C, Sasaki S, Ishii N, Klinman DM, Okuda K, Akira S, Suzuki K (2005) TRAF4 acts as a silencer in TLR-mediated signaling through the association with TRAF6 and TRIF. Eur J Immunol 35:2477–2485.

Terasaki Y, Sasaki T, Yagita Y, Okazaki S, Sugiyama Y, Oyama N, Omura-Matsuoka E, Sakoda S, Kitagawa K (2010) Activation of NR2A receptors induces ischemic tolerance through CREB signaling. J Cereb Blood Flow Metab 30:1441–1449.

Trapp BD, Stys PK (2009) Virtual hypoxia and chronic necrosis of demyelinated axons in multiple sclerosis. Lancet Neurol 8:280–291.

Vadigepalli R, Chakravarthula P, Zak DE, Schwaber JS, Gonye GE (2003) PAINT: a promoter analysis and interaction network generation tool for gene regulatory network identification. OMICS 7:235–252.

Villmann C, Becker CM (2007) On the hypes and falls in neuroprotection: targeting the NMDA receptor. Neuroscientist 13:594–615.

Wang L, Khankhanian P, Baranzini SE, Mousavi P (2011a) iCTNet: a Cytoscape plugin to produce and analyze integrative complex traits networks. BMC Bioinformatics 12:380.

Wang RM, Zhang QG, Li J, Yang LC, Yang F, Brann DW (2009) The ERK5–MEF2C transcription factor pathway contributes to anti-apoptotic effect of cerebral ischemia preconditioning in the hippocampal CA1 region of rats. Brain Res 1255:32–41.

Wang YC, Lin S, Yang QW (2011b) Toll-like receptors in cerebral ischemic inflammatory injury. J Neuroinflammation 8:134.

Wishart DS, Knox C, Guo AC, Cheng D, Shrivastava S, Tzur D, Gautam B, Hassanali M (2008) DrugBank: a knowledgebase for drugs, drug actions and drug targets. Nucleic Acids Res 36:D901–D906.

Yamasaki T, Kawasaki H, Nishina H (2012) Diverse roles of JNK and MKK pathways in the brain. J Signal Transduct 2012:459265.

Zhang B, Kirov S, Snoddy J (2005) WebGestalt: an integrated system for exploring gene sets in various biological contexts. Nucleic Acids Res 33:W741–W748.

Zhang QG, Wang RM, Han D, Yang LC, Li J, Brann DW (2009) Preconditioning neuroprotection in global cerebral ischemia involves NMDA receptor-mediated ERK–JNK3 crosstalk. Neurosci Res 63:205–212.

(Accepted 5 September 2012)
(Available online 15 September 2012)